

**Charles University
1st Faculty of Medicine**

Summary of Ph.D. Thesis
Autoreferát disertační práce



UNIVERZITA KARLOVA
1. lékařská fakulta

Molecular-cytogenetic analysis of aggressive lymphomas

Molekulárně-cytogenetická analýza agresivních lymfomů

MUDr. Jana Karolová

Prague, 07.10.2025

Doktorské studijní programy v biomedicině
Univerzita Karlova a Akademie věd České republiky

Obor: Fyziologie a patofyziologie člověka

Předseda oborové rady: Prof. MUDr. Otomar Kittnar, CSc., MBA

Školící pracoviště: Ústav patologické fyziologie, 1. lékařská fakulta, Univerzita Karlova

Školitel: Prof. MUDr. Pavel Klener, Ph.D.

Disertační práce bude nejméně pět pracovních dnů před konáním obhajoby zveřejněna k nahlížení veřejnosti v tištěné podobě na Oddělení pro vědeckou činnost a zahraniční styky Děkanátu 1. lékařské fakulty.

Doctoral Study Programs in Biomedicine
Charles University and the Czech Academy of Sciences

Field of Study: Human Physiology and Pathophysiology

Chair of the Field Board: Prof. MUDr. Otomar Kittnar, CSc., MBA

Supervising Department: Institute of Pathological Physiology, First Faculty of Medicine, Charles University

Supervisor: Prof. MUDr. Pavel Klener, Ph.D.

The dissertation will be made available for public consultation in printed form at the Department for Research Activities and International Relations of the Dean's Office, First Faculty of Medicine, at least five working days prior to the defense.

CONTENTS

1. Abstract
2. Introduction
3. Hypothesis
4. Aims
5. Materials and Methods
6. Results
 - 6.1. Characteristics of MCL patients and their clinical outcome
 - 6.2. Resulting counts of genomic aberrations, represented by variants, and identified by WES
 - 6.3. Comparison of mutational patterns in diagnostic and corresponding relapsed samples
 - 6.4. Genomic landscape of patients with MCL at diagnosis – analysis of variants and CNV changes
 - 6.5. Genomic landscape of patients with MCL at relapse – analysis of variants and CNV changes
 - 6.6. Establishment of patient-derived xenografts (PDX) of aggressive lymphomas
7. Discussion
8. Conclusion
9. References
10. Supplement: List of publications

1. ABSTRACT

Mantle cell lymphoma (MCL) remains one of the most challenging B-cell lymphomas, known for frequent relapses and poor outcomes in high-risk subgroups. Information about the clonal development of MCL and the genomic landscape of relapsed patients with MCL is still scarce, and such patients are in urgent need of more sophisticated therapies. Additionally, a group of aggressive non-Hodgkin lymphomas (NHLs) still lacks sufficiently effective preclinical models, and their complex characterization is of utmost importance for developing reliable experimental models.

Our whole-exome sequencing study of 25 paired diagnostic and relapse samples from MCL patients treated with standard immunochemotherapy revealed significant clonal evolution during disease progression. Resistant subclones, which were enriched for harmful genetic lesions like *TP53* and *CDKN2A* inactivation, were likely present at diagnosis and selected by therapy. At relapse, these clones exhibited increased genetic diversity, characterized by a higher mutation load, more extensive and numerous copy number alterations, and notably higher variant allele frequencies of *TP53* mutations. We also identified new relapse-associated candidate drivers, including *LRP1B*, *KMT2D*, *SP140*, *NOTCH1/2*, *PIK3CA*, and *GNA14*, highlighting the complexity of clonal dynamics and pointing to potential biological mediators of resistance. These results also underscore the limited effectiveness of chemotherapy in patients with *TP53* and *CDKN2A* inactivation and support early consideration of innovative treatments, such as genetically engineered T-cell immunotherapies, for this high-risk group.

In parallel, we performed a detailed characterization of 15 newly developed patient-derived xenograft (PDX) models of aggressive lymphomas, including MCL, DLBCL, Burkitt lymphoma, and T-cell lymphomas. Whole-exome sequencing confirmed that PDX models accurately preserved the genetic profiles of the original lymphomas, maintaining both mutational patterns and copy number variations. However, detailed histopathological analyses revealed consistent phenotypic differences. PDX tumors showed more aggressive morphology, higher proliferation rates, and a significant reduction in tumor microenvironment (TME) complexity. Notably, human non-malignant immune cells were absent, murine macrophages did not infiltrate the tumors, and vascularization was limited to murine vessels with significantly decreased microvessel density and area compared to the original biopsies. These differences highlight that, while PDXs are highly relevant translational tools, they portray tumors with reduced dependence on human TME components and should be interpreted with caution in

studies focusing on angiogenesis, immune responses, or therapies that depend on the microenvironment.

Taken together, these two complementary studies enhance our understanding of MCL pathogenesis and offer crucial insights for translational lymphoma research. They show how chemotherapy influences clonal evolution by selecting for genetically complex, therapy-resistant subclones, highlighting the need to incorporate new therapeutic strategies into initial treatment plans. Additionally, they demonstrate that PDX models are valuable yet imperfect tools that retain the key genetic features of aggressive lymphomas, albeit in a different microenvironmental context, highlighting both their advantages and limitations for preclinical and clinical studies. Overall, this work offers novel insights into the pathophysiology of MCL and provides a strong foundation for enhancing risk stratification in MCL. Additionally, it increases the translational relevance of experimental models, ultimately supporting the development of more effective treatments for aggressive lymphomas.

Keywords: aggressive lymphomas, mantle cell lymphoma, genomic landscape, clonal development, patient-derived xenografts

2. INTRODUCTION

Aggressive lymphomas are a diverse group of blood cancers characterized by rapid growth and early dissemination of the disease. The most common subtypes mentioned in this study include Diffuse Large B-cell lymphoma (DLBCL), Burkitt lymphoma (BL), T-cell lymphomas (TCL), and Mantle Cell lymphoma (MCL) [1, 2].

MCL in relapsed and refractory cases is a challenging therapeutic hurdle. Its hallmark, translocation t(11;14)(q13;q32), overexpresses cyclin D1, promoting uncontrolled cell cycle progression. Other genetic abnormalities are necessary for further MCL development, and are represented by recurrent changes in *ATM*, *TP53*, *KMT2D*, *NOTCH1*, *NOTCH2*, *RBI*, or *CDKN2A* genes. These aberrations lead to the dysregulation of essential pathways, including the cell cycle, the DNA damage response pathway, and the apoptotic pathway. While the genomic landscape at diagnosis is well-studied, further research is needed on the genetic make-up, clonal development, and disease progression in relapsed cases to identify new therapeutic targets. Especially, *TP53* and *CDKN2A* aberrations often lead to chemoresistance, needing innovative treatment strategies. Next-generation sequencing technologies can provide answers to these questions [3-9].

Patient-derived xenografts (PDX) from patients with aggressive lymphomas serve as effective experimental models in translational research. Since they are used in both preclinical and clinical studies, the genetic and histopathological similarity of these models to the samples they are derived from is crucial for generating reliable data, which can enhance understanding of lymphoma biology and help identify new therapeutic targets. PDXs generally reflect most of the genetic landscape of the patient's disease and, to some extent, also represent the complexity of the tumor microenvironment and the phenotype of the original tumor. However, issues such as the loss of heterogeneity, lack of microenvironmental and immune interactions, or selective bias still exist. Therefore, accurate characterization of PDX models is essential for their future application in translational research, providing reliable experimental tools for understanding disease pathophysiology and developing advanced therapies [10-15].

3. HYPOTHESIS

1. Standard immunochemotherapy drives the clonal evolution of MCL, leading to the expansion of pre-existing genetically diverse subclones and subsequent clinical relapse.
2. PDX models of aggressive lymphomas share the majority of genetic aberrations despite failing to recapitulate the tumor's microenvironment (namely, its non-malignant components).

4. AIMS

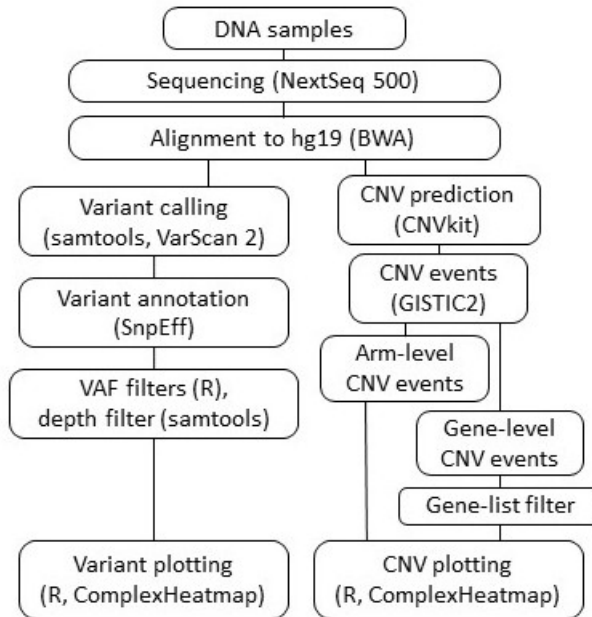
1. To investigate and describe the genomic landscape, molecular features, and clonal evolution of patients with aggressive lymphomas, focusing primarily on those with mantle cell lymphoma, using next-generation sequencing technologies.
2. To characterize the molecular and genetic profiles of PDX models derived from tumor tissues of patients with aggressive lymphomas, and to further validate the relevance of these models for preclinical translational and experimental studies.

5. MATERIALS AND METHODS

The methodology presented here was used in two core publications described in this work (Karolová et al., 2023; Jakša et al., 2022) [16, 17].

Diagnostic, consequent relapsed, and non-malignant samples of 25 patients with MCL were used for the analysis. Infiltration of tumor samples was measured using standard diagnostic workup (Flow cytometry, measured at the Department of Medical Biochemistry and Laboratory Diagnostics at the General University Hospital in Prague, VFN). Only samples with infiltration of 30% or greater were analyzed. Data such as age, sex, MIPI, tumor morphology, Ki-67, initial therapy, autologous stem cell transplantation, best response to treatment, event-free survival (EFS), overall survival (OS), last follow-up date (LFD), or death were used for further analysis and correlation with genomic data.

Samples were homogenized and prepared for DNA isolation as dry pellets, containing $3-5 \times 10^6$ cells. The DNeasy Blood & Tissue Kit (Qiagen, Germany) was used to extract genomic DNA according to the manufacturer's protocol. The quality and concentration of the isolated DNA were measured using a NanoDrop spectrophotometer (Thermo Fisher Scientific, Wilmington, DE, USA). DNA samples were transported to the CLIP facility (Childhood Leukaemia Investigation Prague), Department of Pediatric Hematology and Oncology, 2nd Faculty of Medicine, Charles University, and University Hospital Motol, Prague, Czech Republic. They were sequenced on the NextSeq 500 instrument (Illumina, San Diego, CA), with sequencing libraries prepared using the SureSelect QXT Target Enrichment kit and the SureSelect XT Human All Exon V6+UTR kit (Agilent Technologies, Santa Clara, CA), following the manufacturer's protocol (Agilent Technologies, 2021), SureSelectQXT Target Enrichment for the Illumina Platform Featuring Transposase-Based Library Prep Technology Protocol (Version F2, p/n G9681-90000). The bioinformatics processing of the resulting data is represented in the diagram below. Mutational analysis and copy number variant analysis (CNV) were performed. All filtered variants were manually reviewed using the Integrative Genomic Viewer (IGV).



Overview of data processing during WES analysis. WES = whole exome sequencing, SNV/indel = single nucleotide variations/insertions or deletions, VAF = variant allele frequency, CNV = copy number variations, GISTIC = Genomic Identification of Significant Targets in Cancer.

DNA libraries for capture-based next-generation sequencing (NGS) were prepared using the KAPA HyperPlus Kit (Roche) with KAPA Universal Adaptors (Roche) and KAPA UDI Primer Mixes (Roche), following the manufacturer’s KAPA HyperCap Workflow v3.2 protocol. The validation of CNV events of the *PIK3CA* and *CDKN2A* genes was performed using the TaqMan Copy Number Reference Assay RNase P (ThermoFisher Scientific), according to the manufacturer's instructions. Screen for common genetic abnormalities (*CDKN2A*, *TP53* deletions) at diagnosis was performed using interphase fluorescence in situ hybridization (FISH) analysis as part of standard baseline diagnostic procedures. Statistical analyses were performed with GraphPad version 5 (GraphPad Prism version 5.00 for Windows, GraphPad Software, La Jolla, CA, USA, www.graphpad.com) and with R version 4.2.1 and RStudio 2022.07.1 (R Core Team 2021. R: A language and environment for statistical computing. R Foundation for Statistical Computing, Vienna, Austria, <https://www.R-project.org/>).

Lymphoma samples for the derivation of 15 PDX models of aggressive lymphomas, represented by DLBCL, BL, MCL, and T-NHLs, were obtained using the same principles mentioned above, i.e., from each patient, a diagnostic and non-malignant sample was collected. Tumor samples were homogenized and sorted for CD19- or CD45-positive cells using the

MACS® (Magnetic-Activated Cell Sorting) system (MidiMACS™ Separator, Miltenyi Biotec, Great Britain), following standard protocols. The establishment of PDX models was done using only female immunodeficient mice NOD.CD-Prkdc^{scid} Il2^{rgtm1Wjl}/SzJ, purchased from the Jackson Laboratory in Bar Harbor, Maine, USA. Mice were housed in individually ventilated cages at the Center for Experimental Biomodels, First Faculty of Medicine, Charles University, Prague, Czech Republic. When tumors in the subcutaneously injected mice reached 2 cm in the largest dimension, or when engraftment of tumors in the subrenal capsule became visible by ultrasound examination (Vevo 3100/LAZR-X), the animals were euthanized, and the tumors were used for subsequent analyses. Together with the lymphoma samples from which they were derived, they underwent immunohistochemical analysis, quantification of microvessel density and area, and whole-exome sequencing (WES).

A methodology for WES analysis, adhering to the same principles, is presented above with minor adjustments. Curated gene lists for each lymphoma subtype (DLBCL, MCL, T-NHLs, BL) were created based on recent publications [8, 18-46]. The threshold for variant allele frequency (VAF) of detected mutations in at least one sample was set to a VAF of 10% or greater (20% was used in previous analyses). CNV analysis, completely adhering to the same principles, is visualized above. Variants with copy numbers higher or lower than 2, i.e., amplifications and deletions in selected genes, were plotted for each patient sample and corresponding PDX model using the circlize package for R [47].

Immunohistochemical analysis of patient lymphoma biopsies and their corresponding PDX models, and quantification of microvessel density and microvessel area, was performed by my colleagues. A detailed methodology, along with all necessary citations, is provided in Jakša et al. (2022) [17].

6. RESULTS

6.1. Characteristics of MCL patients and their clinical outcome

In our analysis, 75 % of patients were male, and the age range was between 47 and 81 years (median = 68 years). According to the Mantle Cell Lymphoma International Prognostic Index (MIPI), 84% of patients had high-risk disease, 59% had adverse lymphoma morphology (pleomorphic or blastoid), and 56% had a high proliferation Ki-67 marker ($\geq 30\%$). Patients were treated with R-CHOP-like regimens (56%), 44% received intensified treatments. The response to initial therapy was assessed using computed tomography or PET/CT (positron emission tomography/computed tomography) scans. Out of 25 patients, 23 achieved either complete remission (CR) or partial remission (PR), and stable disease (SD) was observed in two patients. The median EFS for the entire group was 10 months (1.3 – 90.6), and the median OS was 29 months (9.5-109.5).

6.2. Resulting counts of genomic aberrations, represented by variants, and identified by WES

A total of 922 non-synonymous variants were identified; 90% of these were SNVs, the rest were small insertions and deletions. A count of 616/922 variants was shared between diagnostic and relapsed samples; 236 were newly detected (N/D, or gained) at relapse, and 70 variants were newly undetected at diagnosis (N/U, or lost). Comparison of variants (mean \pm SEM) between diagnostic and relapsed samples revealed 24.6 ± 1.7 shared variants, 9.8 ± 1.9 N/D variants, and 3.5 ± 0.8 N/U variants per patient. The number of gained variants at relapsed samples was significantly lower ($p < 0.05$) compared to the number of lost variants at the diagnostic ones (see **Figure 1**). The same conclusion applies when comparing shared with N/D and shared with N/U variants. A significant difference with p -values < 0.001 was observed when comparing the total mean number of variants per patient at relapse (34.1 ± 2.9) and in the diagnostic samples (27.4 ± 1.8). A statistically significant increase was observed in general relapsed samples, with a minority of variants being lost. The majority of variants detected by WES were shared between the diagnostic and relapsed samples.

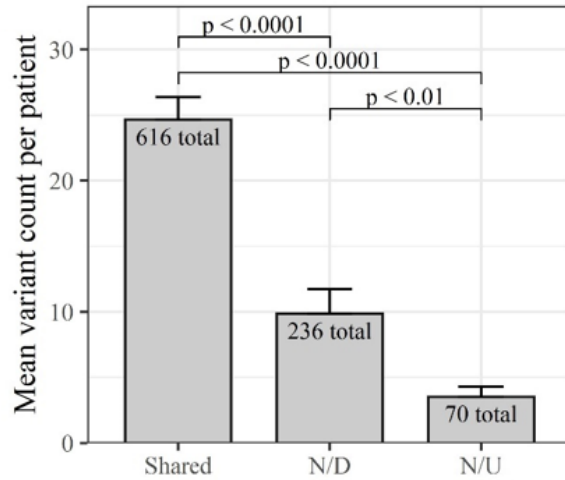


Figure 1: A bar plot, presenting the Mean \pm Standard error of the Mean (SEM) and total variant count of filtered variants, which were shared, N/D, and N/U at relapse and diagnosis. For statistical comparison, we used an unpaired t-test, and p -values were adjusted using the Holm method.

6.3. Comparison of mutational patterns in diagnostic and corresponding relapsed samples

A similar mutational pattern was observed between diagnostic and relapsed samples, as represented by a comparison of percentages of detected variant types in **Table 1**.

Type of variant	Diagnostic sample (%)	Relapsed sample (%)
missense	82.7	83.1
stop-gained	7.1	7.0
frame-shift	6.9	6.6

Table 1: Comparison of percentages of detected variant types.

Diagnostic and relapsed samples harbored substitutions, represented mainly by transitions. Transitions reached 57.3% and 55.2% at diagnostic and relapsed samples, respectively. Transversions were observed in a lower percentage, 33.4% at diagnosis, and 35.9% in relapsed samples. The impact of variants was predicted by the SnpEff toolbox. High-impact and moderate-impact variants that could disrupt gene and protein function were identified. For high-impact variants, such as nonsense or frame-shift mutations, 97 were observed at diagnosis, and 117 at relapse (a 20.6% increase in relapsed samples). The majority of variants had a moderate impact and are represented by missense or in-frame deletions. 583 of them was at diagnosis and 727 at relapse (a 24.7% increase in relapsed samples).

6.4. Genomic landscape of patients with MCL at diagnosis – analysis of variants and CNV changes

The most frequently mutated gene at diagnosis was the tumor suppressor *TP53* (48% of patients). The second was *ATM* (32%), followed by *KMT2D*, *CCND1*, *SP140*, and LDL receptor-related protein 1B (*LRP1B*) genes (28%, 20% for *CCND1* and *SP140*, and 16%, respectively). Another six mutated genes were observed in 12% of patients (*NFKBIE*, *ARFGEF3*, *NOTCH1*, *TRAF2*, *CASP5*, and *SMARCA4*). The spectrum of altered genes comprised 36 additional genes that were mutated in ≥ 2 patients. A total of 12 variants in the *TP53* gene were identified, with 75% located in the p53 DNA binding domain, 17% in the p53 tetramerization domain, and one in the untranslated region.

Analysis of CNV arm-level events identified significant deletions (frequency score > 0.15 , q -value < 0.25) localized to chromosomal arms 9p, 9q, 13q, and 17p, as well as amplification on chromosomal arm 3q. Filtration against our assembled CNV gene list, containing 22 genes, was positive for 20 of the 22 genes, which were deleted or amplified in ≥ 2 patients. Specifically, 50% of patients were positive for deletions of *GNAI4*, 46% had deletions of *TP53*, *ANXA1*, *ALDH1A1*, *MIR15A*, and *MIR16-1*, and 42% harbored deletions of *CDKN2A*, *RBI*, *NOTCH1*, *RHOBTB2*, *SORBS3*, and *TNFRSF10B* genes, respectively. Another 16 genes predicted to have deletions were identified in more than six patients. Amplifications were present in the *PI3K* and *SOX2* genes (46% both). Of note, 37.5% and 20% of patients were positive for amplifications of the *MYC* and *BCL2* genes, respectively. Independent validation of *TP53* deletions was performed using FISH. Verification by FISH was consistent with the WES predicted results in 91% of cases. The *TP53* mutations or deletions were, therefore, detected in 64% of patients, with 29% of them having co-occurrence of both events.

6.5. Genomic landscape of patients with MCL at relapse – analysis of variants and CNV changes

Relapsed samples kept the majority of the variants already identified in the diagnostic samples. *TP53* gene variants were found in 48% of relapsed cases, and all *TP53* variants present at diagnosis were detected at relapse. No new *TP53* mutations appeared in the relapsed samples. Still, a significant increase in the variant allele frequency (VAF) of the known *TP53* variants was observed (median VAF 0.35 at diagnosis and 0.76 at relapse).

Other detected variants in relapsed samples involved mutations in the *ATM* (36%), *KMT2D* (32%), *LRP1B* (24%), *SP140* (20%), and *CCND1* (20%) of patients, with an additional nine genes found in 12% of patients. Several candidate genes in the relapse dataset were newly

discovered, i.e., N/D variants. Three patients carried new variants of the *LRP1B* gene that were absent in their corresponding diagnostic samples, with a total number of *LRP1B* mutations at relapse equal to 6 (24%). Of note, one patient had two *LRP1B* variants. The correlation between *LRP1B* mutation, mutational burden, and overall survival (OS) revealed that relapsed MCL patients with *LRP1B* mutations have a significantly higher mutational burden and display a trend toward decreased OS at diagnosis.

Newly detected variants identified by WES in ≥ 2 two patients at relapse were represented by mutations in the genes *KMT2D*, *HOXD9*, *CDC27*, *RYR2*, and *FLNA*. Variants in five genes, observed at diagnosis in two or more patients (*ATM*, *CASP5*, *ETNK1*, *LRR1Q1*, and *NOTCH2* genes), were also found in one additional case at relapse samples, respectively.

CNV analysis of arm-level chromosomal events revealed that the majority of detected events at diagnosis were present in the relapsed samples, too, except for 1p and 19p chromosomal arm deletions. New arm-level events included one newly gained (7p) and three newly lost chromosomal arms (6q, 8p, 21p). The frequency and magnitude of detected amplifications and deletions at relapse were notably higher, meaning that the amplified and deleted regions had significantly higher weight (p -value < 0.05). We found a similar range of gene deletions and amplifications as described in diagnostic samples; however, the majority of gains and losses observed at diagnosis were more prevalent at relapse. The most frequent predicted abnormality in relapsed samples was the deletion of *CDKN2A* and *CDKN2B* (8 relapsed samples) compared to diagnosis (75% of patients). The presence of *CDKN2A* deletion at diagnosis was associated with overall survival (OS) and was linked to significantly shorter OS (p -value = 0.001).

Deletion of the *TP53* gene was observed in four new cases (a 58% relapse rate and a 12% increase from diagnosis). One patient lost the *TP53* deletion at the relapsed sample. When combined with mutations of the *TP53* gene, inactivation was found in 76% of relapsed samples, with seven patients having both mutation and deletion, five patients having only mutation, and seven patients having only deletion.

Three patients acquired *ATM* deletion at relapse (37.5% of patients). Seven had both deletion and mutation, two had only a mutation, and three had only a deletion. The presence of either an isolated *ATM* mutation or an *ATM* mutation and/or deletion in the diagnostic sample displayed a trend toward increased OS.

We identified several amplified genes in relapsed samples, including *PIK3CA*, *SOX2*, *MYC*, and *BCL2*, in 50%, 46%, 37.5%, and 29% of the samples, respectively. All of them were detected more frequently at relapse than at diagnosis.

Validation of predicted CNV events (*CDKN2A*_{del} and *PIK3CA*_{amp}) at relapse, conducted using the DNA copy number assay TaqMan, revealed a high correlation between predicted CNV events and the TaqMan assay results—specifically, 86% and 88% of samples correlated with predicted *CDKN2A* deletion and *PIK3CA* amplification.

6.6. Establishment of patient-derived xenografts (PDX) of aggressive lymphomas

Fifteen PDX models of aggressive lymphomas were established from diagnostic (5/15) and relapsed (10/15) patient samples. Samples were obtained from seven patients with DLBCL, one patient with transformation of marginal zone lymphoma into DLBCL, one double-hit lymphoma positive for *MYC* and *BCL2* gene rearrangements, one BL, two MCLs, and five (T-NHLs). PDX models (13/15) underwent WES following the principles described above. Two PDX models could not be analyzed due to a lack of available DNA. Analysis confirmed that PDX models retain the majority of somatic variants detected by WES. Analysis of median allele frequencies (VAF) of shared variants confirmed that VAFs in PDX models are similar to those in corresponding lymphoma samples.

A representative example comparing the genetic landscape of a DLBCL patient with his corresponding PDX model is provided below in **Figure 2**. The figure presented below illustrates a complex visualization of the comparison, using a circular ideogram provided in part A of the figure along with predicted CNV events. The outer circular track represents CNV chromosomal positions, while the two inner tracks display the predicted CNVs in specific chromosomal regions of the patient and its established PDX model. At the center of each circular ideogram is a color-coded table, where gene amplifications and deletions specific to each lymphoma subtype are filtered based on our CNV gene lists. Detected amplifications and deletions are highlighted with shades of red and blue, and the numbers of predicted gains and losses (CN = copy number) are shown next to the color-coded table of detected events. Specifically, number two indicates a normal CN, number three indicates a gain of one allele, and a value greater than 3 indicates a gain of more than one allele. The darker the red, the more gains are present. For deletions, number one indicates a predicted monoallelic deletion (lighter blue shade), and number two indicates a predicted biallelic deletion (darker blue shade). Below the circular ideogram in part B, a scatter plot is displayed that shows the VAF of all shared, N/D, and N/U variants of the PDX model compared to the corresponding patients' lymphoma sample. Each

figure comprises a stacked bar plot (part C) of shared, gained (N/D), and lost (N/U) variants between the PDX model and a lymphoma sample, from which it was derived.

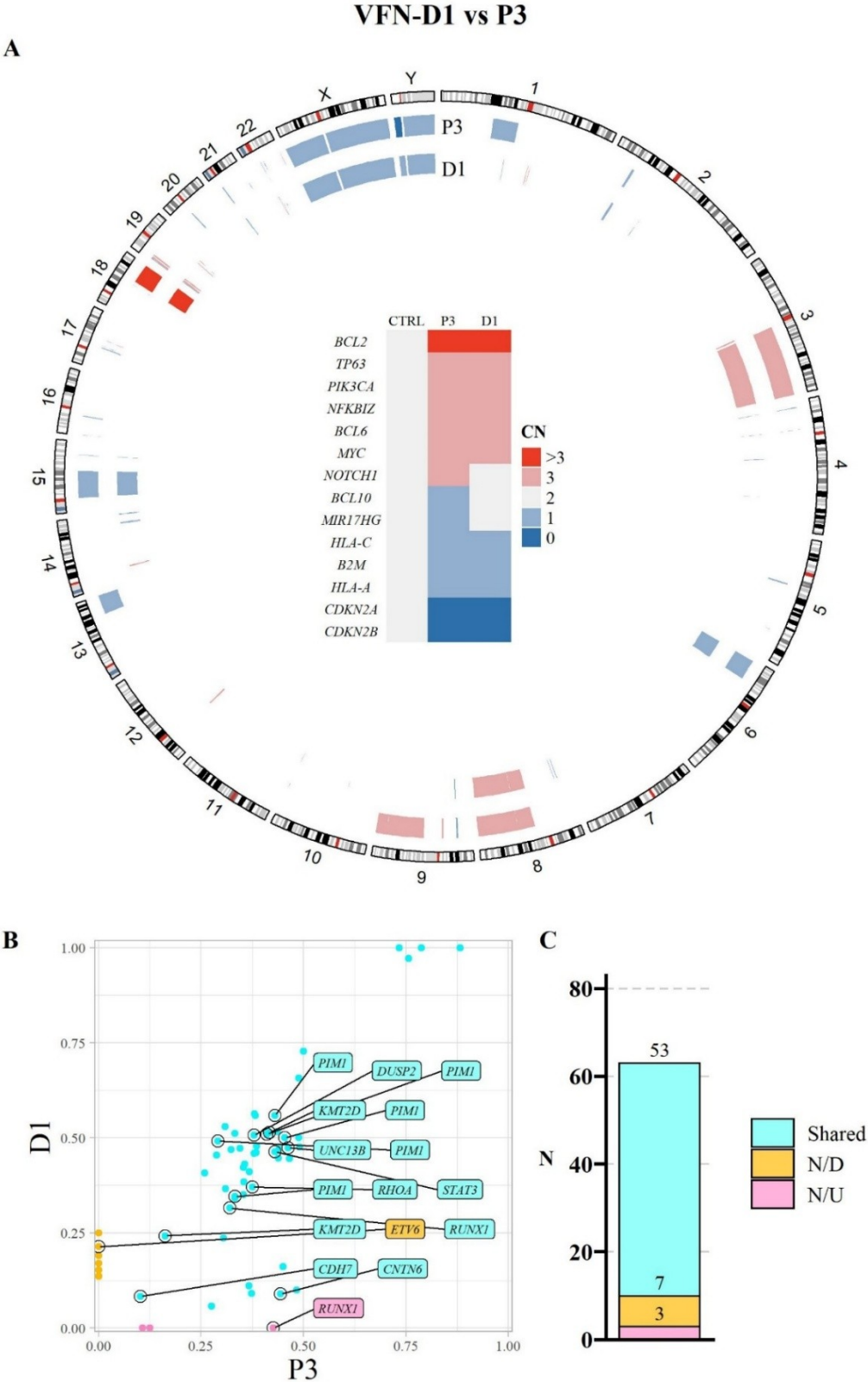


Figure 2: WES analysis of a PDX model VFN-D1, derived from a patient (P3) with DLBCL (non-GC). GC = germinal center. *Reprinted from Jakša et al. (2022).*

An analysis of N/D and N/U variants was conducted, focusing on the distribution of VAFs across patient samples and corresponding PDX models. The list of N/U variants detected in the lymphoma sample but not in the matching PDX model mainly included mutations with low variant allele frequency, with only a small portion of these variants involving genes from the pre-assembled gene lists. The median VAF of N/U variants across all patient samples was 0.15. N/D variants, found in PDX models but not in the matching patient samples, appeared more often than N/U variants, and the majority of them were not detectable in corresponding primary lymphoma samples (VAF in primary sample = 0). In general, most N/D mutations had low VAFs, with a median VAF of 0.18 across all PDX models. Additionally, variants in genes from our pre-assembled lists were more common compared to the N/U variants mentioned earlier. Only a minority of N/D variants were detected below the VAF threshold ($\geq 10\%$) in patient samples. Transitions were the most frequent types of nucleotide substitutions detected in our data set of N/D variants, suggesting that the process of somatic hypermutation may contribute to the establishment and generation of PDX models.

7. DISCUSSION

The mutational profiles of 25 MCL patients were examined, including primary diagnostic samples and corresponding relapsed samples after failure of standard immunochemotherapy used as first-line treatment. Only patients who experienced a disease relapse were included in this analysis. Therefore, this analysis of diagnostic and consequent relapse samples is a rare source of new data, and according to our knowledge, comprises one of the largest cohorts of MCL patients with sequential samples to date [7].

Only patients who experienced relapse were included; therefore, they harbored an increased amount of unfavorable prognostic factors, represented, e.g., by advanced MIPI or an increased rate of *TP53* gene mutations. Specifically, the *TP53* gene in our cohort was the most frequently mutated at diagnosis and detected in 48% of patients. Despite not reaching statistical significance, which could be caused by the relatively small number of cases included in our analysis (25), the occurrence of *TP53* mutation at diagnosis displayed a trend toward decreased OS. As the *TP53* mutation is a critical predictor of poor prognosis in MCL, multiple studies are focusing on developing treatment strategies for patients with this mutation. A recently published systematic review and meta-analysis of patients with newly diagnosed or relapsed/refractory *TP53*-mutated MCLs by Zhang et al. (2025) offers a comprehensive view of the treatment approaches currently employed, including targeted therapy, allogeneic stem cell transplantation, and CAR-T cell therapy [48].

Identified shortened EFS and OS also justified this poor prognosis in our cohort, with durations of 10 and 29 months, respectively. Notably, Sarkozy et al. (2025) recently published a paper analyzing 1280 MCL patients, focusing on patients included in randomized first-line MCL trials conducted in France, for whom progression of disease within two years (POD24) could be evaluated. Patients who relapsed within 24 months had significantly lower post-relapse median OS (9.3 months) compared to those who did not relapse (median OS not reached) or relapsed later (median OS = 49.4 months). A significant association of POD24 with adverse prognostic factors and shortened post-relapse OS mentioned above was identified in this study [49].

Other high-risk events at the CNV level were detected, including arm-level alterations such as del (9p), del (13q), and del (17p). These abnormalities involve crucial genes that play roles in processes like the cell cycle, apoptosis, or the DNA damage response pathway. Notably, deletions of genes such as *CDKN2A*, *CDKN2B*, and *TP53* are among them. This set of aberrations closely resembles those described in the C4 cluster, as noted in the study by Yi et

al. (2022). In that context, the C4 cluster is characterized by the presence of the aforementioned arm-level deletions, along with *TP53* mutations and a hyperproliferative signature, with a 5-year OS of 14.2%. Yi et al. also described cluster C2, which is enriched with *ATM* deletions and mutations, along with upregulated NF- κ B and DNA repair pathways, estimating a 5-year OS of 56.7% [50]. In our study, visualizing the variants detected at diagnosis and relapse revealed two distinct clusters, too: one with *TP53* gene mutations and no *ATM* mutations, and another with *ATM* mutations and no *TP53* mutations. Only one exception with both mutations was found. This may indicate the presence of different biological subgroups within our cohort of MCL cases. Notably, our cohort demonstrated a correlation between *TP53* mutation and a trend toward decreased overall survival, as well as a correlation between *ATM* mutation and a trend toward increased overall survival compared to wild-type individuals. However, also in *ATM*-mutated cases, this did not reach statistical significance. Previous studies have mentioned the mutual exclusivity of these mutations and their distinct clinical impacts. Nevertheless, when additional aberrations are present, such as the co-occurrence of *TP53* and *CDKN2A* alterations, the cumulative effect may be significantly altered [9, 51, 52].

We compared the occurrence of resulting individual aberrations at diagnosis from our data set with current literature and identified a clear enrichment of prognostically adverse variants. Mutations of *TP53* were already mentioned, but increased numbers of mutations of *KMT2D*, *SP140*, or *NOTCH1* and *NOTCH2* were found in 28%, 20%, and 24% (for both *NOTCH1* and *NOTCH2*), respectively, with the previously mentioned deletion of *CDKN2A/2B* predicted in 42% of patients. Notably, mutations in the *TP53*, *KMT2D*, *SP140*, *NOTCH1*, and *NOTCH2* genes were overrepresented in our cohort, in contrast to unselected cohorts of newly diagnosed MCL mentioned in the literature. Conversely, *ATM* mutations accounted for 32%, a proportion lower than that reported in previously published literature. [7, 8, 27-29, 45, 46, 50, 53-55].

Only a small proportion of newly identified variants were found in relapsed samples. We assume that the higher occurrence of known prognostically unfavorable alterations at diagnosis could promote the growth of therapy-resistant clones that lead to relapse. This might, to some extent, explain why fewer de novo mutations are detected in relapsed samples.

The observation that most variants and CNVs present at diagnosis remain at relapse (i.e., shared variants) indicates that core genetic lesions persist throughout the disease course. At the same time, relapse is characterized by the emergence of newly identified mutations along with more numerous and larger CNVs, reflecting a significant increase in the genetic heterogeneity of the chemotherapy-resistant clones. This may occur through two different mechanisms. One is that

chemoimmunotherapy might select for MCL subclones with frequent *TP53* and *CDKN2A/2B* inactivation, which are inherently more heterogeneous at baseline. Alternatively, these clones may acquire additional mutations and CNVs during relapse, as a defective DNA response pathway renders them more susceptible to genomic alterations. Addressing this question will require single-cell omics analyses.

The consequences of an increased mutational burden were discussed in a study by Obr et al. (2020), which examined the prognostic impact of the *TP53* mutational burden (VAF and frequency of del 17p) in a cohort of 114 newly diagnosed MCL patients. Their findings indicate that in younger patients, a high *TP53* mutation burden is predictive of chemoresistance, irrespective of the standard treatment approach [56].

Inactivation of the *TP53* gene, caused by mutations and/or deletions, along with deletions of *CDKN2A/2B*, were the most common abnormalities, detected in 76% and 75% of relapsed samples, respectively. Only two patients did not harbor these aberrations. However, in both cases, mutations in other well-known driver MCL genes were identified—specifically, *KMT2D* and mutations in either *NOTCH1* or *NOTCH2* [55, 57-59].

Although no new variants of the *TP53* gene were found in the relapsed samples, the median VAF of existing *TP53* mutations increased significantly, from 0.35 at diagnosis to 0.76 at relapse. The most likely explanation is the „selective therapeutic pressure“ hypothesis, which favors the survival, expansion, and dissemination of *TP53*-mutated subclones. An alternative explanation („compartment“ hypothesis) is that MCL subclones in different compartments may already show variable *TP53* VAFs at diagnosis. In this scenario, the preferential survival and expansion of cells with higher *TP53* VAFs in a given compartment could account for the elevated VAFs observed at relapse. Targeted sequencing of *TP53* across available compartments in patients P02, P19, and P20 revealed uniformly low VAFs at diagnosis compared to relapse, supporting the selective pressure hypothesis over the compartment hypothesis. In patients P02 and P19, WES identified two additional variants emerging at relapse (*NEGR1* and *EZH2*), which were subsequently added to the targeted sequencing panel. Targeted sequencing verified the presence of both variants in the relapsed samples, whereas they were absent from the corresponding diagnostic samples.

WES analysis predicted new *CDKN2A/2B* deletions in eight patients who had relapsed. However, it should be noted that WES-based CNV predictions may not be as effective in detecting minor subclones (less than 30%) [60]. This finding is consistent with our results from

diagnostic samples, where routine FISH analysis identified more patients with *CDKN2A* inactivation than WES-based CNV predictions (15 versus 10 cases). These CNV results suggest that minor subclones with *CDKN2A* deletions were likely missed by WES at diagnosis, but became detectable at relapse due to therapy-driven selection and expansion of *CDKN2A*-deleted clones. Our findings, combined with previous data, highlight the critical role of *CDKN2A/2B* deletions in conferring chemoresistance and support the view that *CDKN2A/2B* deletions represent later subclonal events, likely arising within *TP53*-mutated MCL clones [9]. Our analysis of WES data (variants and CNVs) indicates that standard front-line immunochemotherapy tends to select for pre-existing MCL (sub)clones with inactivated DNA damage response pathways (*TP53*_{mut/del}, *CDKN2A*_{del}), aligning with previously published research [7, 9, 55, 61].

Along with genetic losses, CNV analysis revealed recurrent amplifications of key oncogenes, including *PIK3CA*, which codes for the p110 α subunit of phosphatidylinositol 3-kinase (PI3K). Amplifications of *PIK3CA* were among the most frequent CNVs, found in 46% of patients at diagnosis and 50% at relapse, aligning with previously published findings [62, 63]. When combined with frequent deletions of *GNAI4* and forkhead box O3 (*FOXO3*) genes, these *PIK3CA* amplifications indicate disruption of the PI3K-AKT pathway in MCL, both at diagnosis and to a greater extent at relapse [64, 65]. Indeed, results from Bettazova et al. (2024) indicate that frequent PI3K pathway aberrations can alter downstream signaling, resulting in decreased dependence on BCR signaling, enhanced metabolic and hypoxic adaptation, and resistance to targeted therapies in MCL [66].

One of the most commonly mutated genes we observed in our dataset of relapsed samples is the low-density lipoprotein receptor-related protein 1B (*LRP1B*), a tumor suppressor. This gene showed abnormal results in six patients, with three new variants appearing in two of them. *LRP1B* ranks among the most frequently altered genes in human cancers [67-72]. Our results also demonstrated a correlation between *LRP1B* mutation and increased mutational burden in our MCL patients, which has been reported in the literature for other malignancies [71, 73, 74]. *LRP1B* mutations have been connected to poorer overall survival in primary gastrointestinal DLBCL [68]. Our analysis also observed a link between *LRP1B* mutations at diagnosis and shorter OS, though limited by the small number of patients affected (n = 3). While *LRP1B* is acknowledged as an established tumor suppressor gene, its exact role in MCL biology and its potential as a biomarker for prognosis or prediction still requires clarification in larger patient cohorts and functional translational studies.

KMT2D mutations, present in a significant portion of diagnostic samples and newly emerging in two patients at relapse (8 of 25 relapse cases, 32% overall), have likewise been associated with poor prognosis in MCL, as noted above. Besides *LRP1B* and *KMT2D*, we identified multiple other candidate genes newly gained in at least two relapse samples (*HOXD9*, *CDC27*, *RYR2*, and *FLNA*). These genes have been linked to various cancers, but their ability to promote MCL progression remains uncertain [75-79].

The section below will discuss the results observed during the genetic characterization of PDX models.

To evaluate the genomic and histopathologic characteristics of fifteen newly established PDX models, an integrated genetic and histopathological analysis was performed. PDX models of aggressive lymphomas were compared with their corresponding primary tumor biopsies. Our cohort of PDX models included all major aggressive NHL subtypes, represented by GC- and non-GC DLBCL, double-hit and transformed DLBCL, MCL, BL, PTCL, AITL, ALCL ALK-positive, and ALCL-ALK negative lymphomas. WES demonstrated that the PDX models largely preserved the somatic mutations and copy number alterations present in the primary lymphoma cells, which is consistent with previously published findings [14, 15, 80, 81].

Our PDX models closely mirrored primary lymphomas in both the overall number of somatic mutations and the allele frequencies of these mutations. We also observed similar mutational landscapes and predicted CNV profiles between PDXs and their matched primary samples. The WES results suggest that most established PDXs retained their genetic diversity, rather than just representing subclones of the more diverse primary tumors. In most PDXs we analyzed, the number of shared mutations exceeded the combined counts of N/D and N/U variants. Across nearly all models, N/D mutations outnumbered N/U mutations significantly. Notably, most N/D mutations were absent from the corresponding primary lymphoma samples (VAF = 0) and were predominantly nucleotide transitions. These findings indicate that most N/D mutations likely arose de novo during sustained proliferation of PDX cells in the murine host, possibly driven by ongoing somatic hypermutation, which aligns with previous reports [82, 83]. On the other hand, most N/U mutations were likely „lost“ due to the underrepresentation of disease subclones with low-frequency bystander mutations during PDX propagation in the murine organism. Overall, these findings align with previous reports and emphasize both the accuracy and the dynamic evolution of PDX models in vivo [84].

Below, a brief discussion of the results of histopathological analyses, mentioned explicitly in the paper by Jakša et al. (2022) and carried out by my colleagues, follows to provide a full context for the detected changes in our PDX models [17].

Despite largely preserved genetic profiles, histopathological analyses (conducted by my colleagues) revealed that PDX tumors often exhibited more aggressive features than their corresponding primary lymphomas, including higher proliferation rates (Ki-67). PDX tumors lacked human non-malignant cells and murine macrophages, and exhibited significantly reduced microvessel density and area compared to the original biopsies, with vessels of exclusively murine origin. The vascular differences likely result from suboptimal stimulation of murine angiogenesis by human VEGF. They may have important implications for interpreting preclinical studies of anti-angiogenic therapies or drugs that rely on passive tumor accumulation, such as liposomal cytostatics. Beyond changes in the tumor microenvironment, PDX cells also exhibited immunophenotypic anomalies, including decreased *SOX11* and cyclin D1 expression in MCL models, as well as alterations in the expression of cytotoxic granules and markers (CD20, CD3) in specific T-NHL models. Notably, reduced cyclin D1 expression in MCL PDXs compared with primary samples has also been reported by Zhang et al [80]. The PDX models in this study preserved the genetic profiles of the primary lymphomas but lost their tumor microenvironment heterogeneity, likely due to selection for tumors less dependent on human tumor microenvironment components; this aligns with our engraftment rates of only 25-30% over a decade of efforts. Notably, even successfully established PDX cells could not be expanded *ex vivo*, indicating a reliance on *in vivo* growth conditions, which may include cell-to-cell interactions, hypoxia, metabolic demands, or other factors.

8. CONCLUSIONS

Our WES analysis of sequential MCL samples, obtained from diagnosis and subsequent relapses, revealed significant clonal evolution of MCL after failure of standard first-line immunochemotherapy. The data suggest that chemotherapy-resistant (sub)clones, enriched with aberrations in genes with adverse prognostic significance, were likely present at diagnosis in most, if not all, patients. At relapse, these resistant populations were characterized not only by frequent inactivation of key regulators of DNA damage response pathways (notably *TP53* and *CDKN2A/2B*) but also by markedly increased genetic heterogeneity, including more variants and larger CNVs compared with their diagnostic counterparts. These findings highlight the limited effectiveness of chemotherapy in patients with *TP53* and *CDKN2A* inactivation (the so-called C4 cluster disease, described above) and support early use of innovative therapy strategies in this high-risk subgroup, such as immunotherapies with genetically modified autologous T-cells. Additionally, we identified several candidate drivers of MCL relapse, including *LRP1B*, *KMT2D*, *SP140*, *NOTCH1*, *NOTCH2*, *PIK3CA*, and *GNAI4*, which require further investigation in proof-of-concept translational studies to elucidate their biological roles and potential therapeutic applications. Overall, our results provide a framework for enhancing risk stratification in MCL and underscore the pressing need for innovative treatment strategies that can overcome chemotherapy resistance and clonal diversification.

To conclude the analysis of patient-derived xenografts, PDX models are among the most relevant and versatile tools available for translational research. They offer unique opportunities for preclinical evaluation of new therapeutic strategies and functional studies of lymphoma biology. Notably, our findings highlight that although PDX models of aggressive lymphomas do not fully replicate the complexity of primary tumors, particularly regarding histopathological features and tumor microenvironment, they closely mirror and preserve their genomic complexity and heterogeneity. These discrepancies, if ignored, may lead to significant biases in experimental results and their interpretation. Future translational studies should therefore include detailed genetic and phenotypic characterization of PDX models along with complementary experimental systems, with the ultimate goal of enhancing their predictive accuracy for clinical and preclinical applications.

9. REFERENCES

1. Lenz, G. and L.M. Staudt, *Aggressive Lymphomas*. New England Journal of Medicine, 2010. **362**(15): p. 1417-1429.
2. Ribeiro, M.L., et al., *Epigenetic targets in B- and T-cell lymphomas: latest developments*. *The Adv Hematol*, 2023. **14**: p. 20406207231173485.
3. Silkenstedt, E., K. Linton, and M. Dreyling, *Mantle cell lymphoma - advances in molecular biology, prognostication and treatment approaches*. *Br J Haematol*, 2021. **195**(2): p. 162-173.
4. Harmanen, M., et al., *Survival of patients with mantle cell lymphoma in the rituximab era: Retrospective binational analysis between 2000 and 2020*. *Br J Haematol*, 2023. **201**(1): p. 64-74.
5. Eyre, T.A., C.Y. Cheah, and M.L. Wang, *Therapeutic options for relapsed/refractory mantle cell lymphoma*. *Blood*, 2022. **139**(5): p. 666-677.
6. Jares, P., D. Colomer, and E. Campo, *Molecular pathogenesis of mantle cell lymphoma*. *The Journal of clinical investigation*, 2012. **122**(10): p. 3416-3423.
7. Hill, H.A., et al., *Genetic mutations and features of mantle cell lymphoma: a systematic review and meta-analysis*. *Blood Adv*, 2020. **4**(13): p. 2927-2938.
8. Beà, S., et al., *Landscape of somatic mutations and clonal evolution in mantle cell lymphoma*. *Proceedings of the National Academy of Sciences*, 2013. **110**(45): p. 18250-18255.
9. Malarikova, D., et al., *Concurrent TP53 and CDKN2A gene aberrations in newly diagnosed mantle cell lymphoma correlate with chemoresistance and call for innovative upfront therapy*. *Cancers*, 2020. **12**(8): p. 2120.
10. Jin, J., et al., *Challenges and Prospects of Patient-Derived Xenografts for Cancer Research*. *Cancers (Basel)*, 2023. **15**(17).
11. Sugimoto, K., et al., *Discovery of a drug targeting microenvironmental support for lymphoma cells by screening using patient-derived xenograft cells*. *Scientific Reports*, 2015. **5**(1): p. 13054.
12. Byrne, A.T., et al., *Interrogating open issues in cancer precision medicine with patient-derived xenografts*. *Nature Reviews Cancer*, 2017. **17**(4): p. 254-268.
13. Townsend, E.C., et al., *The public repository of xenografts enables discovery and randomized phase II-like trials in mice*. *Cancer cell*, 2016. **29**(4): p. 574-586.
14. Forde, S., et al., *Paediatric Burkitt lymphoma patient-derived xenografts capture disease characteristics over time and are a model for therapy*. *Br J Haematol*, 2021. **192**(2): p. 354-365.
15. Chapuy, B., et al., *Diffuse large B-cell lymphoma patient-derived xenograft models capture the molecular and biological heterogeneity of the disease*. *Blood, The Journal of the American Society of Hematology*, 2016. **127**(18): p. 2203-2213.
16. Karolová, J., et al., *Sequencing-based analysis of clonal evolution of 25 mantle cell lymphoma patients at diagnosis and after failure of standard immunochemotherapy*. *American journal of hematology*, 2023. **98**(10): p. 1627-1636.
17. Jakša, R., et al., *Complex genetic and histopathological study of 15 patient-derived xenografts of aggressive lymphomas*. *Laboratory Investigation*, 2022. **102**(9): p. 957-965.
18. Schmitz, R., et al., *Genetics and pathogenesis of diffuse large B-cell lymphoma*. *New England journal of medicine*, 2018. **378**(15): p. 1396-1407.
19. Pasqualucci, L. and R. Dalla-Favera, *Genetics of diffuse large B-cell lymphoma*. *Blood, The Journal of the American Society of Hematology*, 2018. **131**(21): p. 2307-2319.
20. Reddy, A., et al., *Genetic and functional drivers of diffuse large B cell lymphoma*. *Cell*, 2017. **171**(2): p. 481-494. e15.
21. Dubois, S., et al., *Next-generation sequencing in diffuse large B-cell lymphoma highlights molecular divergence and therapeutic opportunities: a LYSA study*. *Clinical cancer research*, 2016. **22**(12): p. 2919-2928.

22. Karube, K., et al., *Integrating genomic alterations in diffuse large B-cell lymphoma identifies new relevant pathways and potential therapeutic targets*. *Leukemia*, 2018. **32**(3): p. 675-684.
23. Pasqualucci, L., et al., *Analysis of the coding genome of diffuse large B-cell lymphoma*. *Nature genetics*, 2011. **43**(9): p. 830-837.
24. Zhang, J., et al., *Genetic heterogeneity of diffuse large B-cell lymphoma*. *Proceedings of the National Academy of Sciences*, 2013. **110**(4): p. 1398-1403.
25. Lohr, J.G., et al., *Discovery and prioritization of somatic mutations in diffuse large B-cell lymphoma (DLBCL) by whole-exome sequencing*. *Proceedings of the National Academy of Sciences*, 2012. **109**(10): p. 3879-3884.
26. Morin, R.D., et al., *Frequent mutation of histone-modifying genes in non-Hodgkin lymphoma*. *Nature*, 2011. **476**(7360): p. 298-303.
27. Zhang, J., et al., *The genomic landscape of mantle cell lymphoma is related to the epigenetically determined chromatin state of normal B cells*. *Blood, The Journal of the American Society of Hematology*, 2014. **123**(19): p. 2988-2996.
28. Yang, P., et al., *Genomic landscape and prognostic analysis of mantle cell lymphoma*. *Cancer gene therapy*, 2018. **25**(5): p. 129-140.
29. Wu, C., et al., *Genetic heterogeneity in primary and relapsed mantle cell lymphomas: Impact of recurrent CARD11 mutations*. *Oncotarget*, 2016. **7**(25): p. 38180.
30. Crescenzo, R., et al., *Convergent mutations and kinase fusions lead to oncogenic STAT3 activation in anaplastic large cell lymphoma*. *Cancer cell*, 2015. **27**(4): p. 516-532.
31. Larose, H., et al., *Whole exome sequencing reveals NOTCH1 mutations in anaplastic large cell lymphoma and points to Notch both as a key pathway and a potential therapeutic target*. *Haematologica*, 2020. **106**(6): p. 1693.
32. Odejide, O., et al., *A targeted mutational landscape of angioimmunoblastic T-cell lymphoma*. *Blood, The Journal of the American Society of Hematology*, 2014. **123**(9): p. 1293-1296.
33. Palomero, T., et al., *Recurrent mutations in epigenetic regulators, RHOA and FYN kinase in peripheral T cell lymphomas*. *Nature genetics*, 2014. **46**(2): p. 166-170.
34. Sakata-Yanagimoto, M., et al., *Somatic RHOA mutation in angioimmunoblastic T cell lymphoma*. *Nature genetics*, 2014. **46**(2): p. 171-175.
35. Vallois, D., et al., *Activating mutations in genes related to TCR signaling in angioimmunoblastic and other follicular helper T-cell-derived lymphomas*. *Blood, The Journal of the American Society of Hematology*, 2016. **128**(11): p. 1490-1502.
36. Watatani, Y., et al., *Molecular heterogeneity in peripheral T-cell lymphoma, not otherwise specified revealed by comprehensive genetic profiling*. *Leukemia*, 2019. **33**(12): p. 2867-2883.
37. Dave, S.S., et al., *Molecular diagnosis of Burkitt's lymphoma*. *New England Journal of Medicine*, 2006. **354**(23): p. 2431-2442.
38. Love, C., et al., *The genetic landscape of mutations in Burkitt lymphoma*. *Nature genetics*, 2012. **44**(12): p. 1321-1325.
39. López, C., et al., *Genomic and transcriptomic changes complement each other in the pathogenesis of sporadic Burkitt lymphoma*. *Nature communications*, 2019. **10**(1): p. 1459.
40. Panea, R.I., et al., *The whole-genome landscape of Burkitt lymphoma subtypes*. *Blood, The Journal of the American Society of Hematology*, 2019. **134**(19): p. 1598-1607.
41. Penther, D., et al., *A recurrent clonally distinct Burkitt lymphoma case highlights genetic key events contributing to oncogenesis*. *Genes, Chromosomes and Cancer*, 2019. **58**(8): p. 595-601.
42. *Recurrent mutation of the ID3 gene in Burkitt lymphoma identified by integrated genome, exome and transcriptome sequencing*. *Nature genetics*, 2012. **44**(12): p. 1316-1320.
43. Schmitz, R., et al., *Burkitt lymphoma pathogenesis and therapeutic targets from structural and functional genomics*. *Nature*, 2012. **490**(7418): p. 116-120.
44. Wagener, R., et al., *The mutational landscape of Burkitt-like lymphoma with 11q aberration is distinct from that of Burkitt lymphoma*. *Blood, The Journal of the American Society of Hematology*, 2019. **133**(9): p. 962-966.

45. Ahmed, M., et al., *Gene mutations and actionable genetic lesions in mantle cell lymphoma*. *Oncotarget*, 2016. **7**(36): p. 58638.
46. Royo, C., et al. *The complex landscape of genetic alterations in mantle cell lymphoma*. in *Seminars in cancer biology*. 2011. Elsevier.
47. Gu, Z., et al., "*Circlize*" implements and enhances circular visualization in R. 2014.
48. Zhang, N., et al., *Treatment outcomes for patients with newly diagnosed or relapsed/refractory TP53-mutated mantle cell lymphoma: a systematic review and meta-analysis*. *EClinicalMedicine*, 2025. **85**.
49. Sarkozy, C., et al., *Validation of POD24 as a robust early clinical indicator of poor survival in mantle cell lymphoma from 1280 patients on clinical trials, a LYSA study*. *Blood Cancer Journal*, 2025. **15**(1): p. 78.
50. Yi, S., et al., *Genomic and transcriptomic profiling reveals distinct molecular subsets associated with outcomes in mantle cell lymphoma*. *J Clin Invest*, 2022. **132**(3).
51. Greiner, T.C., et al., *Mutation and genomic deletion status of ataxia telangiectasia mutated (ATM) and p53 confer specific gene expression profiles in mantle cell lymphoma*. *Proc Natl Acad Sci U S A*, 2006. **103**(7): p. 2352-7.
52. Mareckova, A., et al., *ATM and TP53 mutations show mutual exclusivity but distinct clinical impact in mantle cell lymphoma patients*. *Leukemia & Lymphoma*, 2019. **60**(6): p. 1420-1428.
53. Salaverria, I., et al., *Specific secondary genetic alterations in mantle cell lymphoma provide prognostic information independent of the gene expression-based proliferation signature*. *J Clin Oncol*, 2007. **25**(10): p. 1216-22.
54. Beà, S., et al., *Increased number of chromosomal imbalances and high-level DNA amplifications in mantle cell lymphoma are associated with blastoid variants*. *Blood*, 1999. **93**(12): p. 4365-74.
55. Ferrero, S., et al., *KMT2D mutations and TP53 disruptions are poor prognostic biomarkers in mantle cell lymphoma receiving high-dose therapy: a FIL study*. *Haematologica*, 2019. **105**(6): p. 1604.
56. Obr, A., et al., *A high TP53 mutation burden is a strong predictor of primary refractory mantle cell lymphoma*. *Br J Haematol*, 2020. **191**(5): p. e103-e106.
57. Kridel, R., et al., *Whole transcriptome sequencing reveals recurrent NOTCH1 mutations in mantle cell lymphoma*. *Blood*, 2012. **119**(9): p. 1963-1971.
58. Silkenstedt, E., et al., *Notch1 signaling in NOTCH1-mutated mantle cell lymphoma depends on Delta-Like ligand 4 and is a potential target for specific antibody therapy*. *Journal of Experimental & Clinical Cancer Research*, 2019. **38**(1): p. 446.
59. Deshotels, L., F.M. Safa, and N.S. Saba, *NOTCH Signaling in Mantle Cell Lymphoma: Biological and Clinical Implications*. *Int J Mol Sci*, 2023. **24**(12).
60. Sandmann, S., et al., *CopyDetective: Detection threshold-aware copy number variant calling in whole-exome sequencing data*. *Gigascience*, 2020. **9**(11): p. giaa118.
61. Eskelund, C.W., et al., *TP53 mutations identify younger mantle cell lymphoma patients who do not benefit from intensive chemoimmunotherapy*. *Blood, The Journal of the American Society of Hematology*, 2017. **130**(17): p. 1903-1910.
62. Psyrrri, A., et al., *Phosphatidylinositol 3'-kinase catalytic subunit α gene amplification contributes to the pathogenesis of mantle cell lymphoma*. *Clinical Cancer Research*, 2009. **15**(18): p. 5724-5732.
63. Iyengar, S., et al., *P110 α -mediated constitutive PI3K signaling limits the efficacy of p110 δ -selective inhibition in mantle cell lymphoma, particularly with multiple relapse*. *Blood*, 2013. **121**(12): p. 2274-2284.
64. Obrador-Hevia, A., et al., *The tumour suppressor FOXO3 is a key regulator of mantle cell lymphoma proliferation and survival*. *British journal of haematology*, 2012. **156**(3): p. 334-345.

65. Xu, C., et al., *GNA14's interaction with RACK1 inhibits hepatocellular carcinoma progression through reducing MAPK/JNK and PI3K/AKT signaling pathway*. *Carcinogenesis*, 2021. **42**(11): p. 1357-1369.
66. Bettazova, N., et al., *Impact of PIK3CA gain and PTEN loss on mantle cell lymphoma biology and sensitivity to targeted therapies*. *Blood Advances*, 2024. **8**(20): p. 5279-5289.
67. Príncipe, C., et al., *LRP1B: a giant lost in cancer translation*. *Pharmaceuticals*, 2021. **14**(9): p. 836.
68. Li, S.-S., et al., *Whole-exome sequencing analysis identifies distinct mutational profile and novel prognostic biomarkers in primary gastrointestinal diffuse large B-cell lymphoma*. *Experimental Hematology & Oncology*, 2022. **11**(1): p. 71.
69. Cascione, L., et al., *Novel insights into the genetics and epigenetics of MALT lymphoma unveiled by next generation sequencing analyses*. *Haematologica*, 2019. **104**(12): p. e558.
70. González-Rincón, J., et al., *Unraveling transformation of follicular lymphoma to diffuse large B-cell lymphoma*. *PLoS One*, 2019. **14**(2): p. e0212813.
71. Zhang, R., et al., *Whole-exome sequencing revealed the mutational profiles of primary central nervous system lymphoma*. *Clinical Lymphoma Myeloma and Leukemia*, 2023. **23**(4): p. 291-302.
72. Schaffer, M., et al., *Activity of ibrutinib plus R-CHOP in diffuse large B-cell lymphoma: response, pharmacodynamic, and biomarker analyses of a phase Ib study*. *Cancer Treatment and Research Communications*, 2020. **25**: p. 100235.
73. Liu, F., et al., *LRP1B mutation: a novel independent prognostic factor and a predictive tumor mutation burden in hepatocellular carcinoma*. *Journal of Cancer*, 2021. **12**(13): p. 4039.
74. Chen, H., et al., *Association of LRP1B mutation with tumor mutation burden and outcomes in melanoma and non-small cell lung cancer patients treated with immune check-point blockades*. *Frontiers in immunology*, 2019. **10**: p. 1113.
75. Zhu, H., et al., *HOXD9 promotes the growth, invasion and metastasis of gastric cancer cells by transcriptional activation of RUFY3*. *Journal of Experimental & Clinical Cancer Research*, 2019. **38**(1): p. 412.
76. Song, Y., et al., *CDC27 promotes tumor progression and affects PD-L1 expression in T-cell lymphoblastic lymphoma*. *Frontiers in Oncology*, 2020. **10**: p. 488.
77. Xu, N., et al., *Low expression of ryanodine receptor 2 is associated with poor prognosis in thyroid carcinoma*. *Oncology Letters*, 2019. **18**(4): p. 3605-3612.
78. Wang, A., et al., *Role and mechanism of FLNa and UCP2 in the development of cervical cancer*. *Oncology Reports*, 2020. **44**(6): p. 2656-2668.
79. Nagasaka, M., et al., *The deubiquitinating enzyme USP17 regulates c-Myc levels and controls cell proliferation and glycolysis*. *FEBS letters*, 2022. **596**(4): p. 465-478.
80. Zhang, L., et al., *B-Cell Lymphoma Patient-Derived Xenograft Models Enable Drug Discovery and Are a Platform for Personalized Therapy*. *Clin Cancer Res*, 2017. **23**(15): p. 4212-4223.
81. Woo, X.Y., et al., *Conservation of copy number profiles during engraftment and passaging of patient-derived cancer xenografts*. *Nature Genetics*, 2021. **53**(1): p. 86-99.
82. Choi, Y.Y., et al., *Establishment and characterisation of patient-derived xenografts as preclinical models for gastric cancer*. *Scientific reports*, 2016. **6**(1): p. 22172.
83. Di Noia, J.M. and M.S. Neuberger, *Molecular mechanisms of antibody somatic hypermutation*. *Annu. Rev. Biochem.*, 2007. **76**(1): p. 1-22.
84. Ben-David, U., et al., *Patient-derived xenografts undergo mouse-specific tumor evolution*. *Nature genetics*, 2017. **49**(11): p. 1567-1575.

10. SUPPLEMENT: List of publications related to the publication

- 1) **Karolová J**, Kazantsev D, Svatoň M, Tušková L, Forsterová K, Maláriková D, Benešová K, Heizer T, Dolníková A, Klánová M, Winkovska L, Svobodová K, Hojný J, Krkavcová E, Froňková E, Zemanová Z, Trněný M, Klener P. Sequencing-based analysis of clonal evolution of 25 mantle cell lymphoma patients at diagnosis and after failure of standard immunochemotherapy. *Am J Hematol.* 2023 Oct;98(10):1627-1636. doi: 10.1002/ajh.27044. Epub 2023 Aug 21. PMID: 37605345. **JIF 2023: 10.1**
- 2) Jakša R, **Karolová J**, Svatoň M, Kazantsev D, Grajciarová M, Pokorná E, Tonar Z, Klánová M, Winkowska L, Maláriková D, Vočková P, Forsterová K, Renešová N, Dolníková A, Nožičková K, Dundr P, Froňková E, Trněný M, Klener P. Complex genetic and histopathological study of 15 patient-derived xenografts of aggressive lymphomas. *Lab Invest.* 2022 Sep;102(9):957-965. doi: 10.1038/s41374-022-00784-w. Epub 2023 Jan 4. PMID: 36775424. **JIF 2022: 5.0**

Other:

- 3) Sun K, Jin L, **Karolová J**, Vorwerk J, Hailfinger S, Opalka B, Zapukhlyak M, Lenz G, Khandanpour C. Combination Treatment Targeting mTOR and MAPK Pathways Has Synergistic Activity in Multiple Myeloma. *Cancers (Basel).* 2023 Apr 19;15(8):2373. doi: 10.3390/cancers15082373. PMID: 37190302; PMCID: PMC10136620. **JIF 2023: 4.5**
- 4) Klanova M, Kazantsev D, Pokorna E, Zikmund T, **Karolova J**, Behounek M, Renesova N, Sovilj D, Kelemen CD, Helman K, Jaks R, Havranek O, Andera L, Trneny M, Klener P. Anti-apoptotic MCL1 Protein Represents Critical Survival Molecule for Most Burkitt Lymphomas and BCL2-negative Diffuse Large B-cell Lymphomas. *Mol Cancer Ther.* 2022 Jan;21(1):89-99. doi: 10.1158/1535-7163.MCT-21-0511. Epub 2021 Nov 2. PMID: 34728569; PMCID: PMC9398137. **JIF 2022: 5.7**
- 5) Pola R, Pokorná E, Vočková P, Böhmová E, Pechar M, **Karolová J**, Pankrác J, Šefc L, Helman K, Trněný M, Etrych T, Klener P. Cytarabine nanotherapeutics with increased stability and enhanced lymphoma uptake for tailored highly effective therapy of mantle cell lymphoma. *Acta Biomater.* 2021 Jan 1;119:349-359. doi: 10.1016/j.actbio.2020.11.014. Epub 2020 Nov 11. PMID: 33186784. **JIF 2021: 10.633**
- 6) Lemm EA, Valle-Argos B, Smith LD, Richter J, Gebreselassie Y, Carter MJ, **Karolova J**, Svaton M, Helman K, Weston-Bell NJ, Karydis L, Williamson CT, Lenz G, Pettigrew J, Harwig C, Stevenson FK, Cragg M, Forconi F, Steele AJ, Cross J, Mackenzie L, Klener P, Packham G. Preclinical Evaluation of a Novel SHIP1 Phosphatase Activator for Inhibition of PI3K Signaling in Malignant B Cells. *Clin Cancer Res.* 2020 Apr 1;26(7):1700-1711. doi: 10.1158/1078-0432.CCR-19-2202. Epub 2019 Dec 12. PMID: 31831562; PMCID: PMC7124891. **JIF 2020: 12.531**

- 7) Pytlik R, Polgarova K, **Karlova J**, Klener P. Current Immunotherapy Approaches in Non-Hodgkin Lymphomas. *Vaccines (Basel)*. 2020 Nov 27;8(4):708. doi: 10.3390/vaccines8040708. PMID: 33260966; PMCID: PMC7768428. **JIF 2020: 4.422**
- 8) Vockova P, Svaton M, **Karlova J**, Pokorna E, Vokurka M, Klener P. Anti-CD38 Therapy with Daratumumab for Relapsed/Refractory CD20-Negative Diffuse Large B-Cell Lymphoma. *Folia Biol (Praha)*. 2020;66(1):17-23. PMID: 32512655. **JIF 2020: 0.906**
- 9) **Karlova J**, Radek M, Helman K, Spacek M, Trneny M, Klener P. PD-1, PD-L1 and PD-L2 Expression in Mantle Cell Lymphoma and Healthy Population. *Folia Biol (Praha)*. 2020;66(4):117-122. PMID: 33745258. **JIF 2020: 0.906**
- 10) Prukova D, Andera L, Nahacka Z, **Karlova J**, Svaton M, Klanova M, Havranek O, Soukup J, Svobodova K, Zemanova Z, Tuskova D, Pokorna E, Helman K, Forsterova K, Pacheco-Blanco M, Vockova P, Berkova A, Fronkova E, Trneny M, Klener P. Cotargeting of BCL2 with Venetoclax and MCL1 with S63845 Is Synthetically Lethal In Vivo in Relapsed Mantle Cell Lymphoma. *Clin Cancer Res*. 2019 Jul 15;25(14):4455-4465. doi: 10.1158/1078-0432.CCR-18-3275. Epub 2019 Apr 19. PMID: 31004002. **JIF 2019: 10.107**
- 11) Klimova A, Heissigerova J, Rihova E, Brichova M, Pytlik R, Spicka I, Mrazova K, **Karlova J**, Svozilkova P. Combined treatment of primary vitreoretinal lymphomas significantly prolongs the time to first relapse. *Br J Ophthalmol*. 2018 Nov;102(11):1579-1585. doi: 10.1136/bjophthalmol-2017-311574. Epub 2018 Jan 29. PMID: 29378728. **JIF 2018: 3.615**